

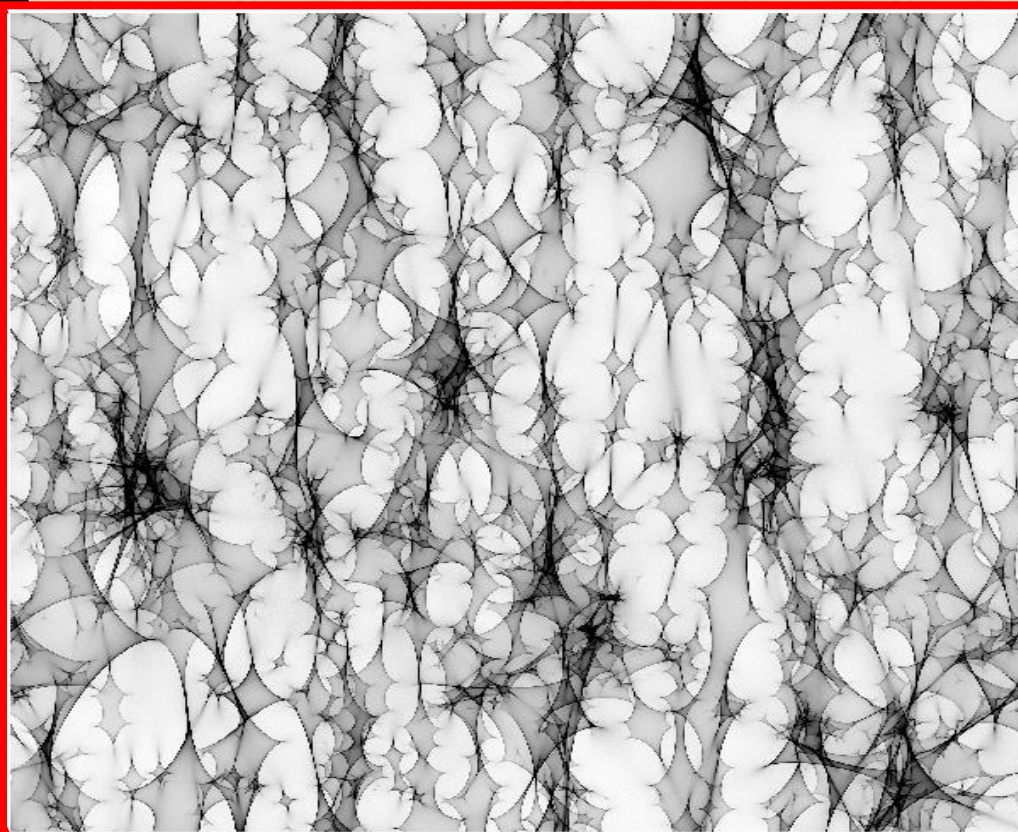
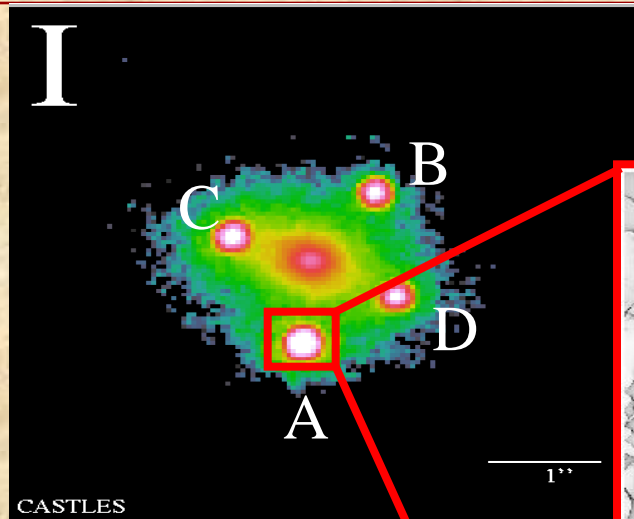
Microlensing Constraints on Quasar X-ray Emission Regions

Xinyu Dai (Univ. of Oklahoma)

- Bin Chen (Univ. of Oklahoma)
- Chris Kochanek (Ohio State Univ.)
- George Chartas (College of Charleston)
- Chris Morgan (Naval Academy)
- Jeff Blackburne (Ohio State Univ.)
- Ana Mosquera (Ohio State Univ.)
- E. Baron (Univ. of Oklahoma)
- R. Kantowski (Univ. of Oklahoma)

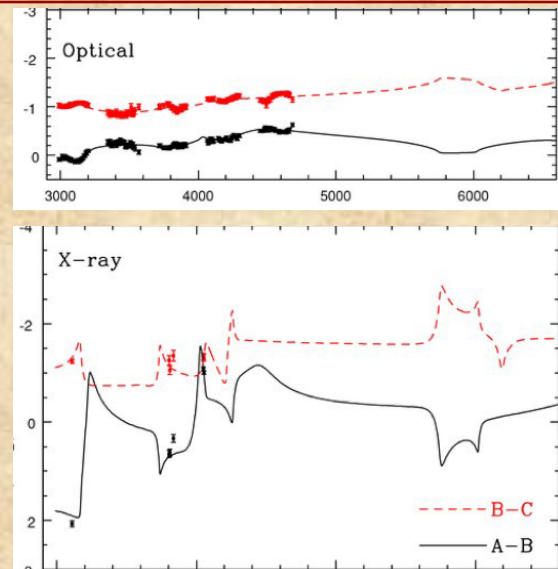
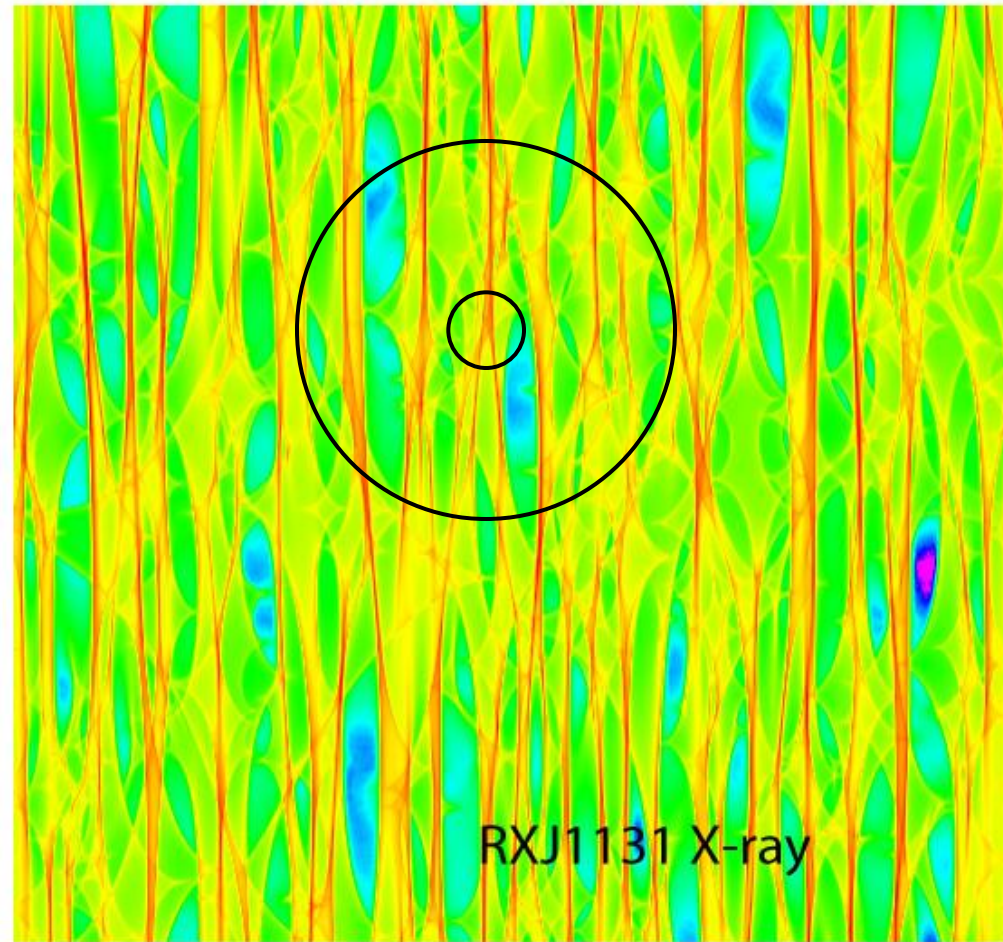


Quasar Microlensing



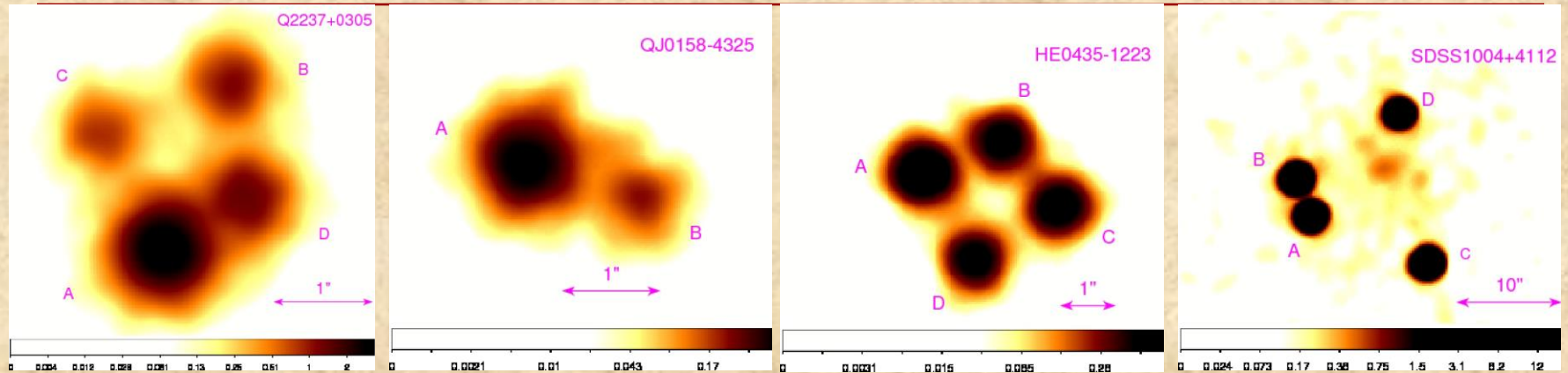
$$\alpha = \frac{4GM}{c^2 \xi}$$

How to use microlensing to measure the source size? — Qualitative Approach



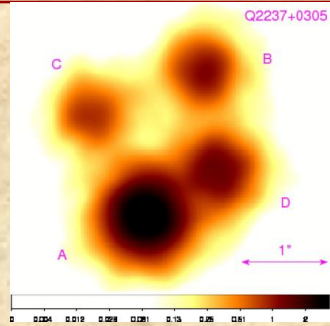
- **Larger sources** smooth the magnification pattern and have **smaller microlensing variability**.

Chandra Monitoring of Gravitational Lenses



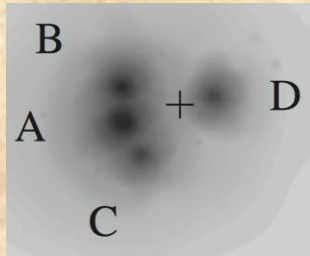
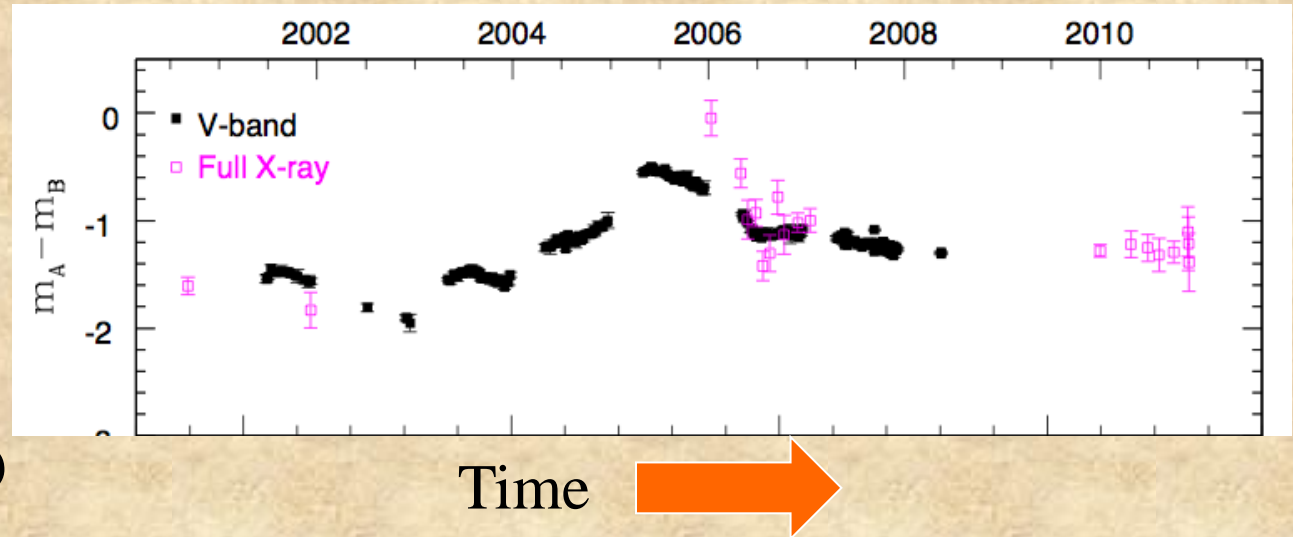
- Chandra resolves the lens images in X-rays
- ~20 lenses with total exp of ~1.5 Ms
- 7 lenses are intensely monitored in our Cycle 11 program ~700 ks.
- Ongoing Cycle 14/15 large program (800 ks, 6 lenses)

X-ray and Optical Microlensing Variability

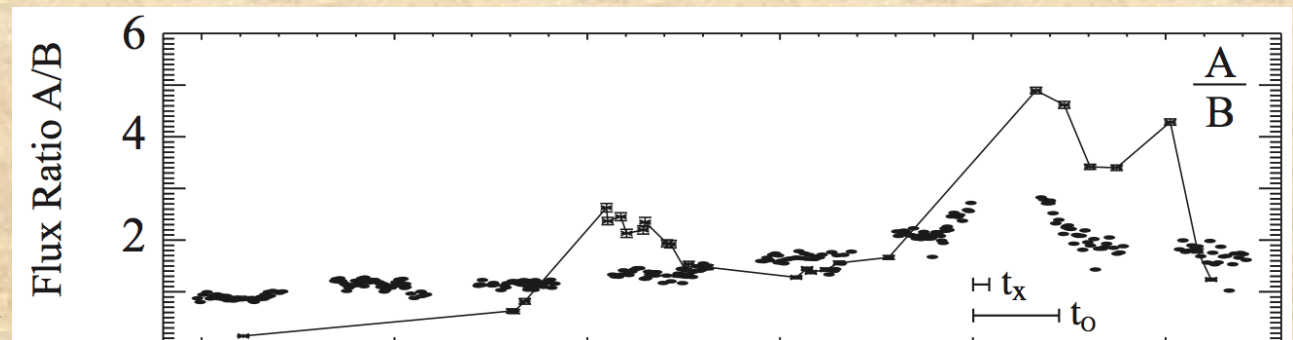


Q2237, Chen et al.
(2011, 2012);

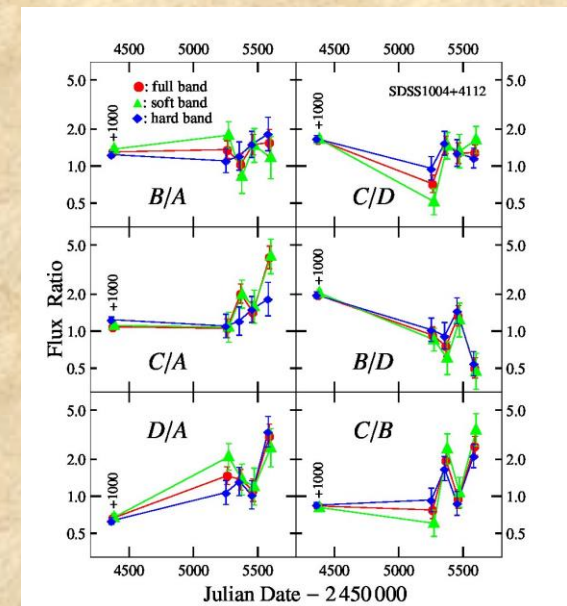
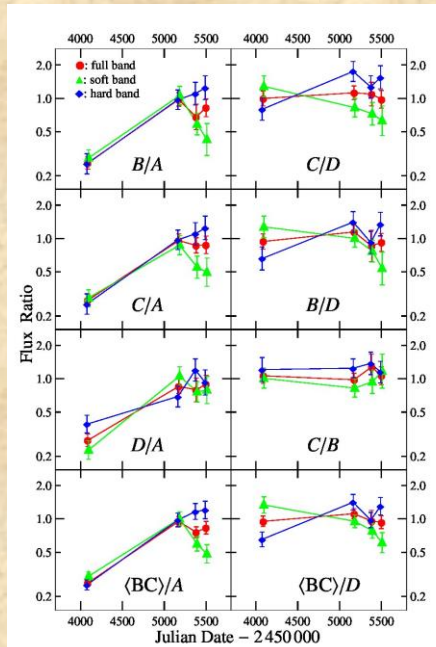
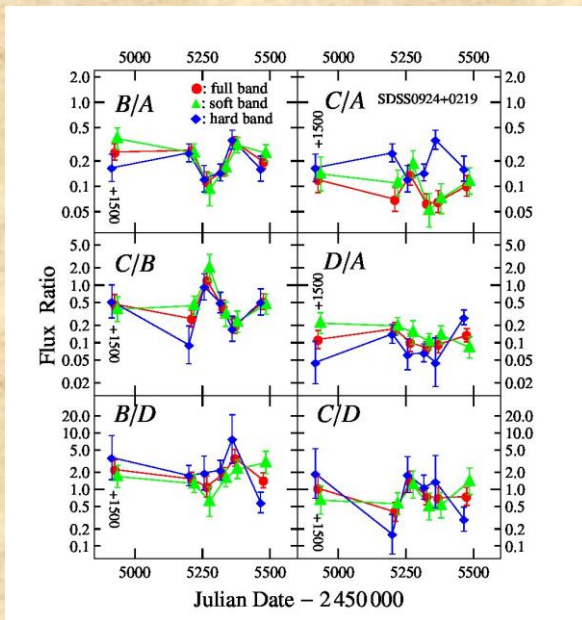
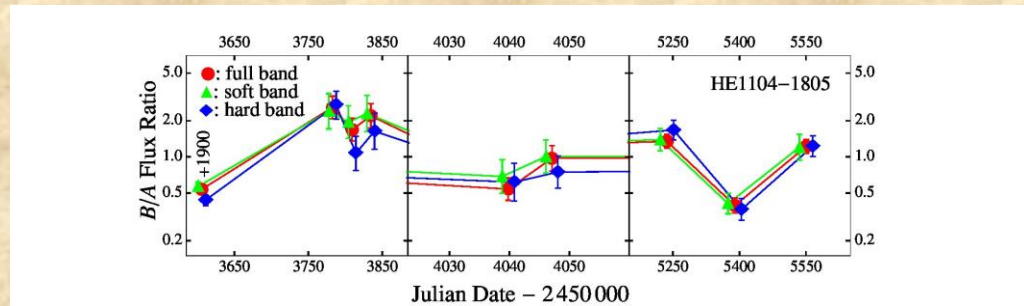
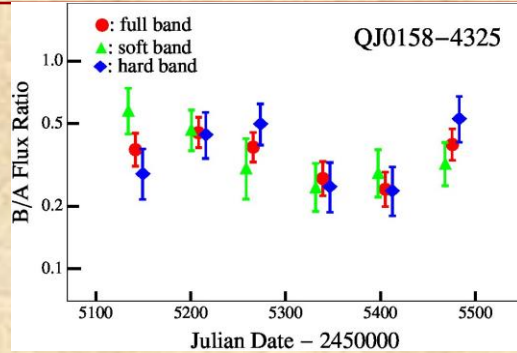
Mosquera et al. (2013)



RXJ1131, Chartas et al. (2012)



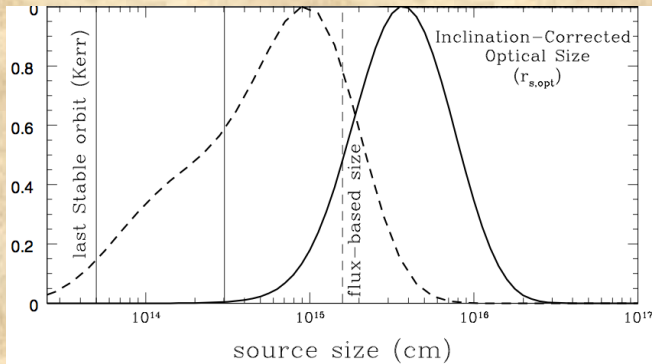
X-ray Microlensing Light Curves (Chen et al. 2012)



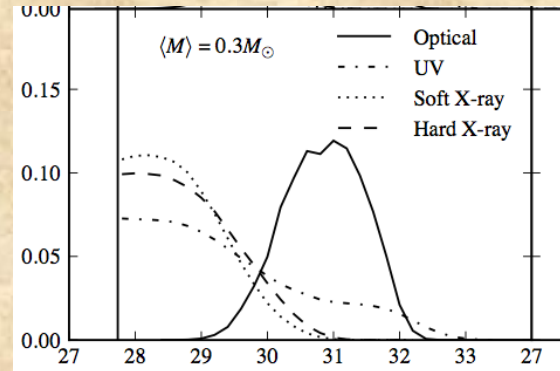
X-ray and Optical Emission Sizes



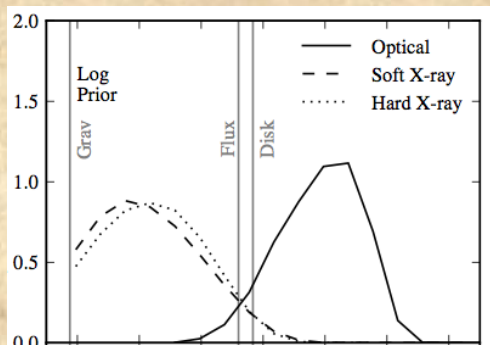
Probability



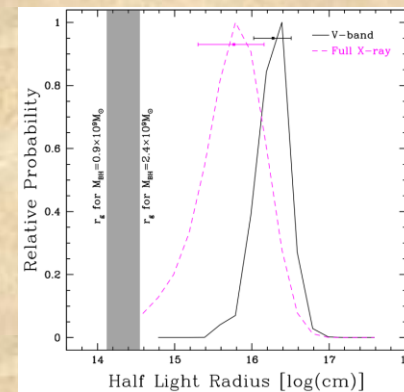
QJ0158, Morgan et al. (2012)



HE0435, Blackburne et al. (2011)

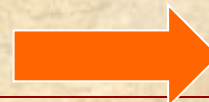


HE1104, Blackburne et al. (2013)

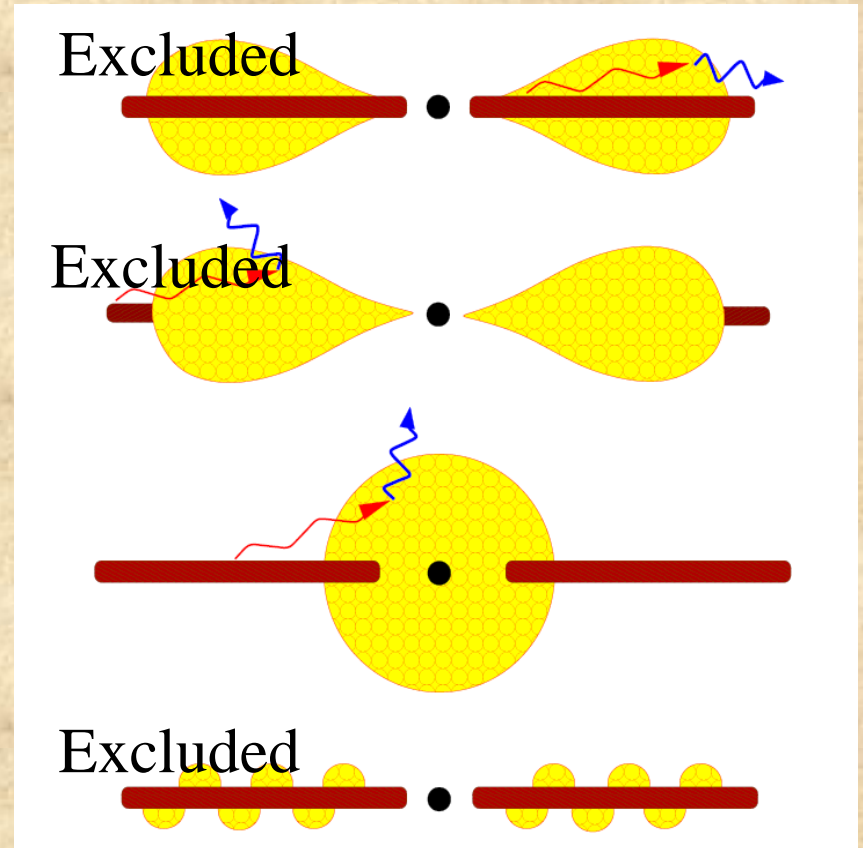
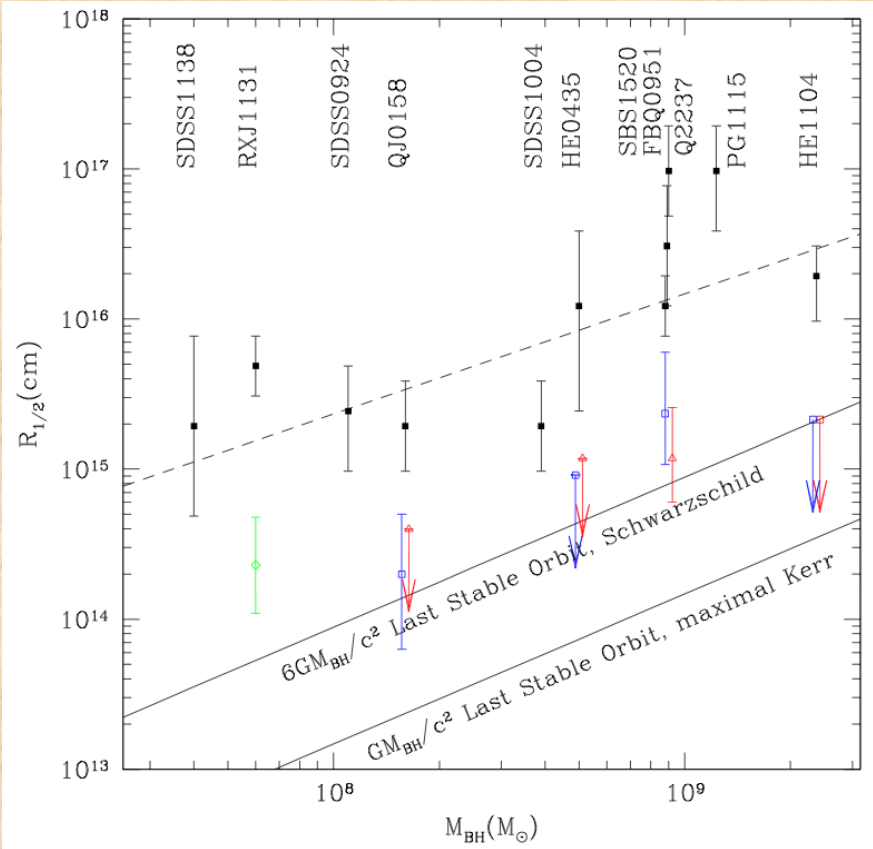


Q2237, Mosquera et al. (2013)

Size

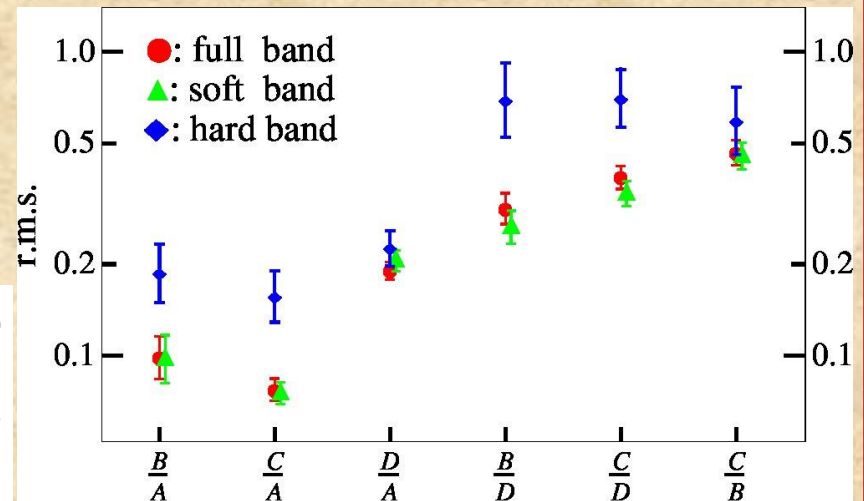
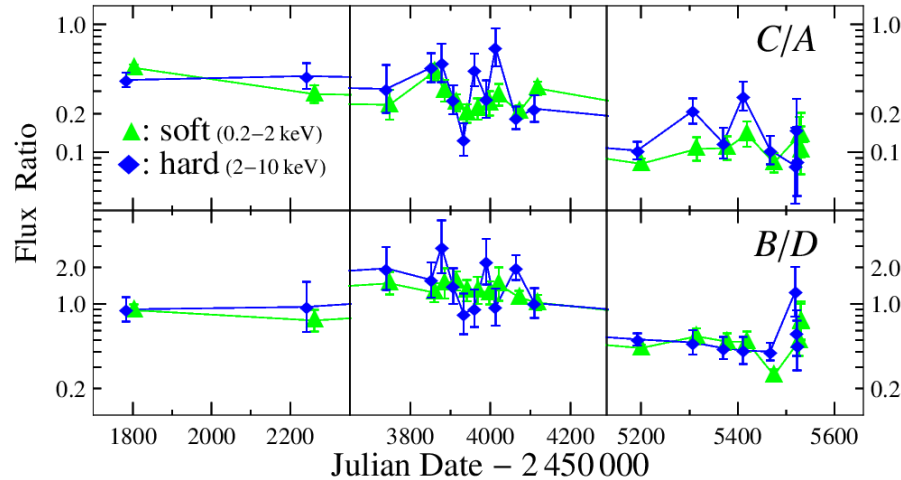
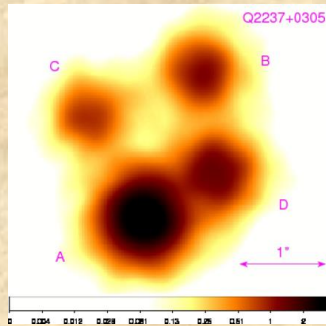


X-ray and Optical Emission Sizes



Energy Dependent X-Ray Microlensing

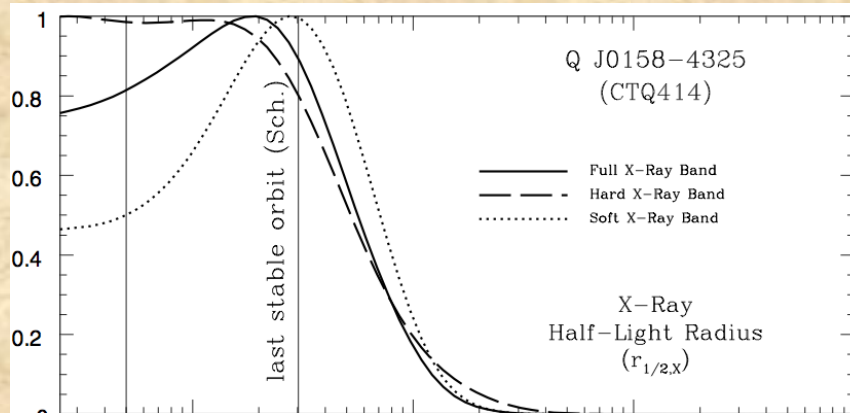
■ Q2237



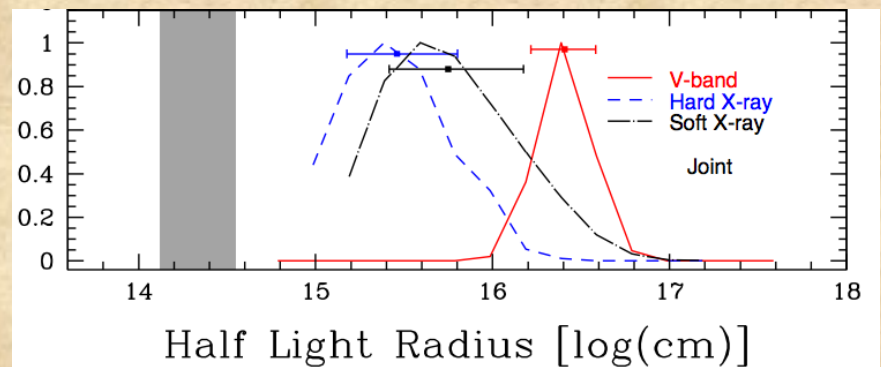
- Larger microlensing variability in hard band.
- Smaller hard source
- Temperature gradient in corona

Chen et al. 2011, ApJL, 740, 34

Energy Dependent X-ray Microlensing



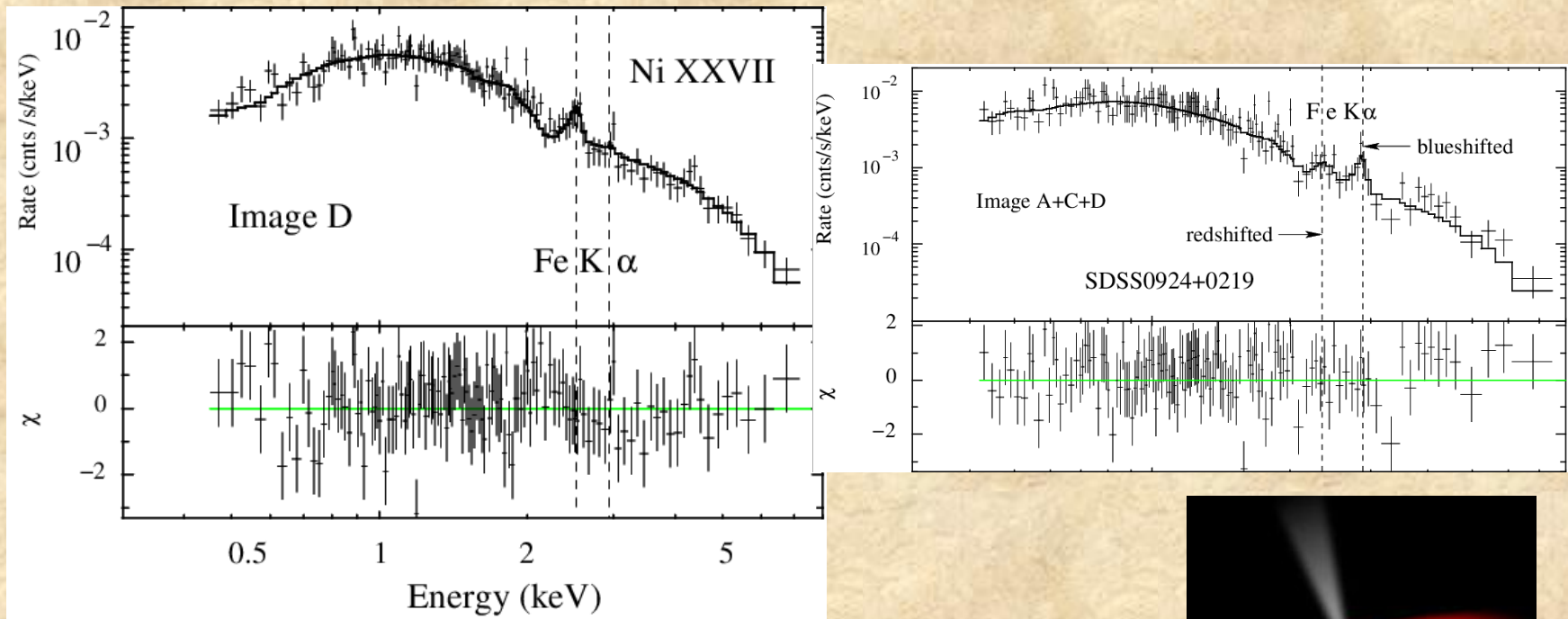
QJ0158, Morgan et al. (2012)



Q2237, Mosquera et al. (2013)

- Hard X-ray Smaller in 2 cases (QJ0158, Q2237).
- Consistent in 2 cases (could due to S/N)
- Hard X-ray larger in one case (RXJ1131).

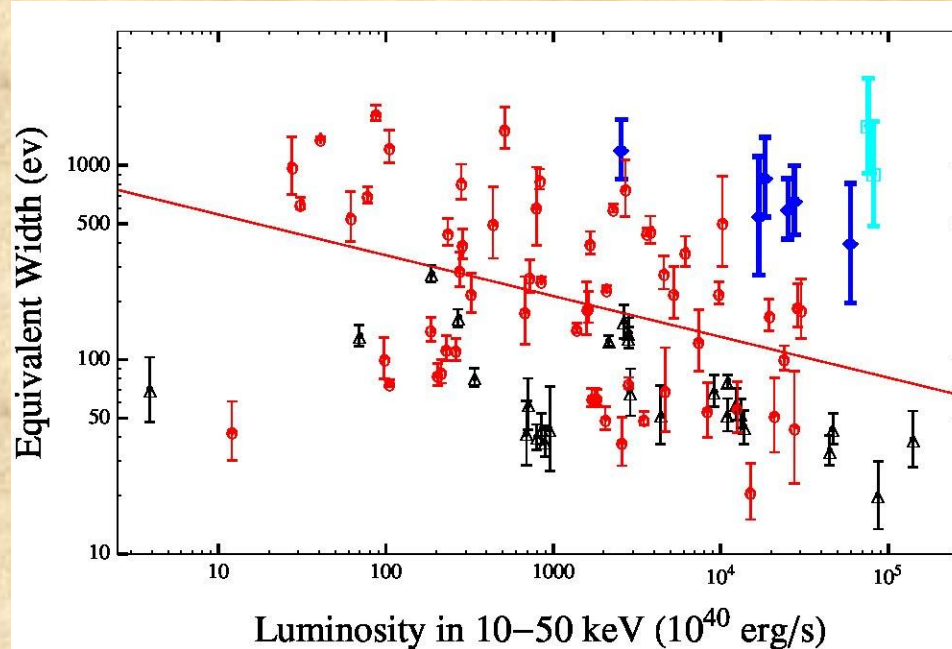
Microlensing of Iron Lines (Chen et al. 2012a)



- Fe Lines are observed in almost all case.
- Sometime we see split of the line.



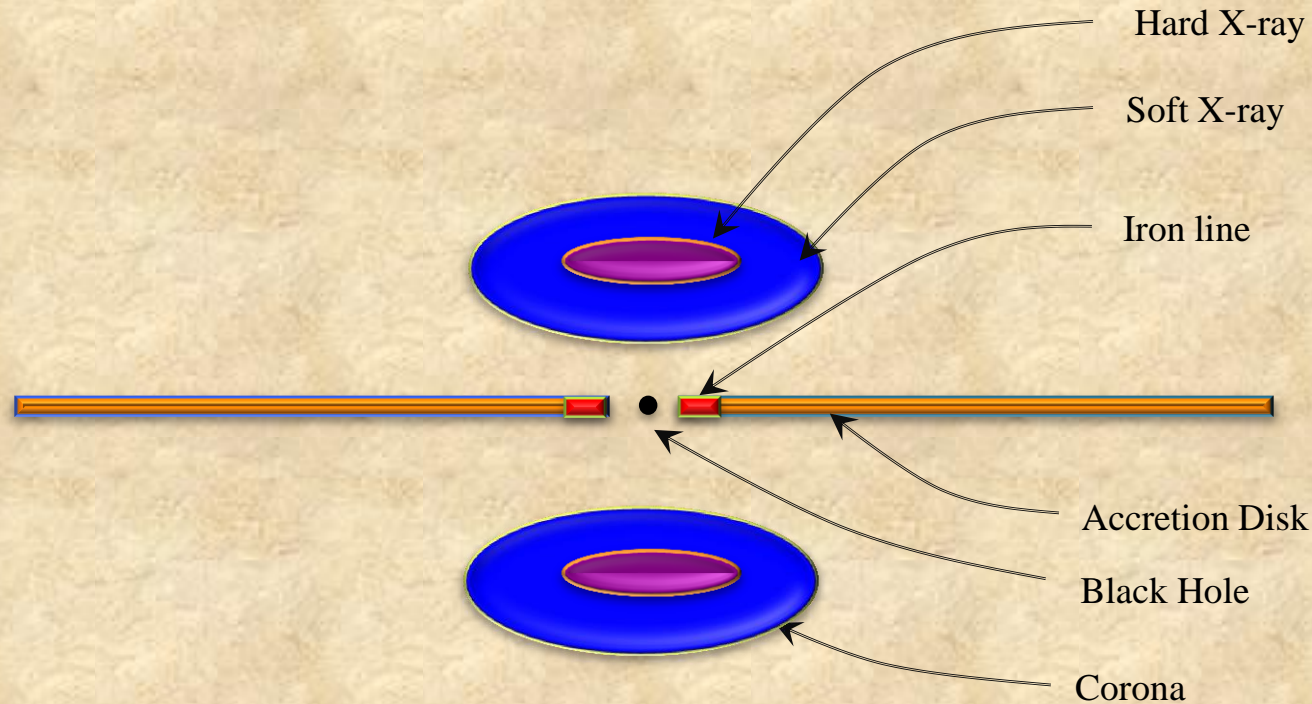
Micro lensing of Iron Lines



Chen et al.
(2012a)

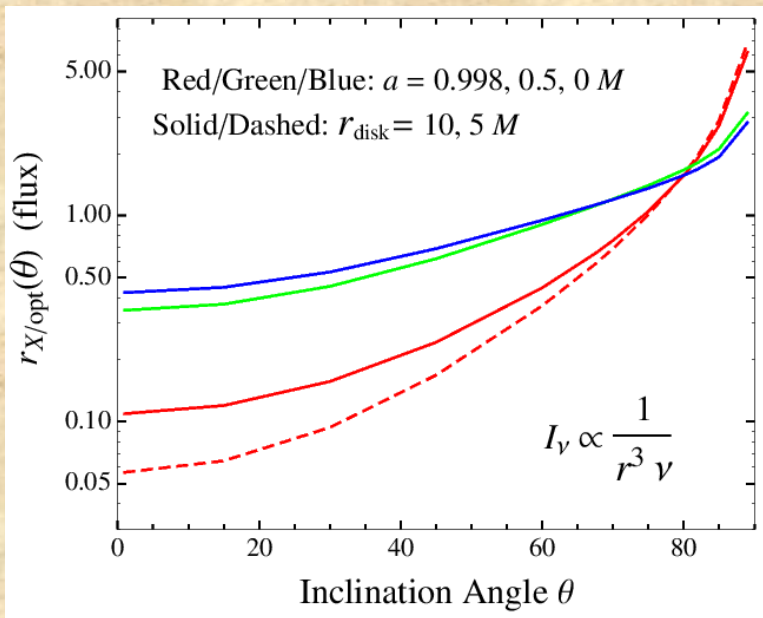
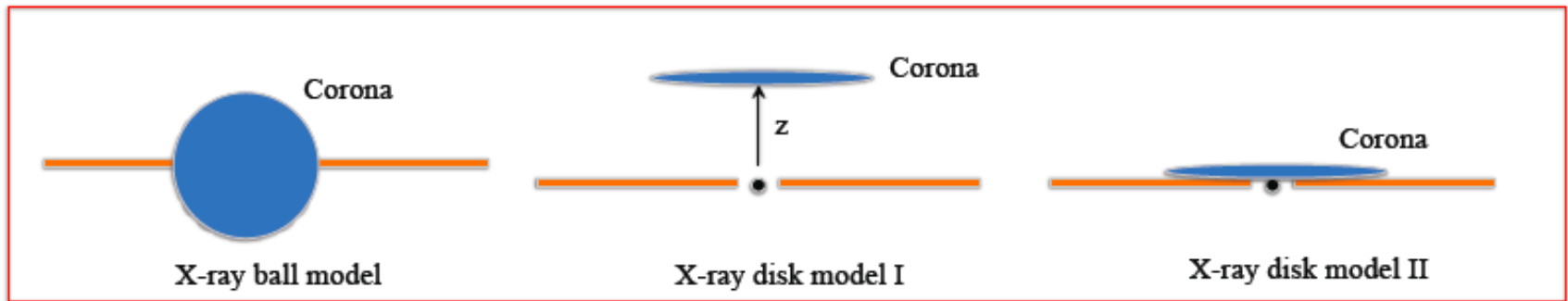
- Iron line EWs in lensed quasars are larger than those of normal AGN of same luminosities.
- Iron line size is even smaller than X-ray continuum.

Model of AGN Accretion Disk



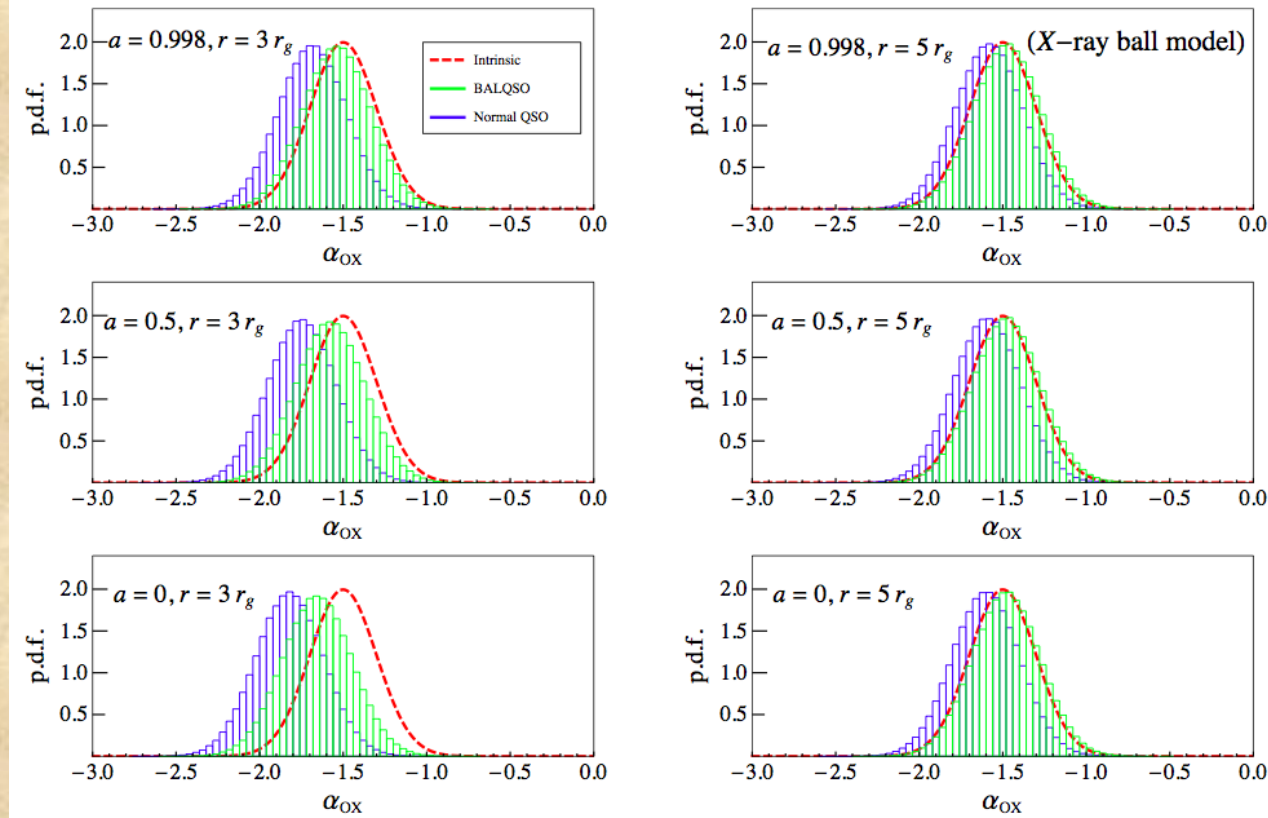
- Cycle 14/15 800 ks program.
- Calibrating all data from Cycle 1 to 15.

X-ray Emission Under Strong Gravity



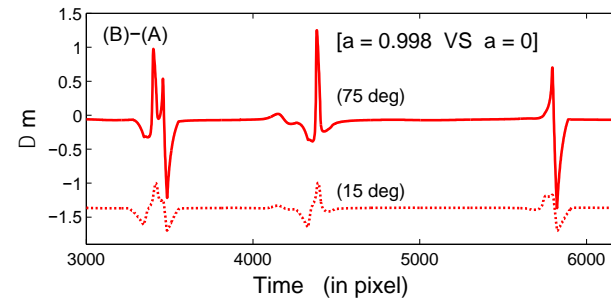
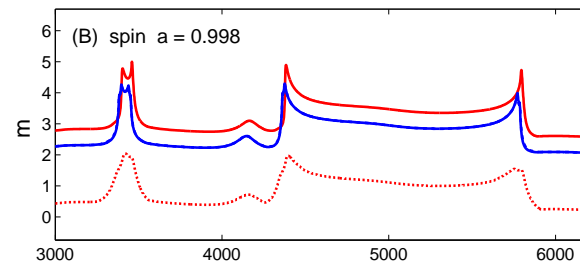
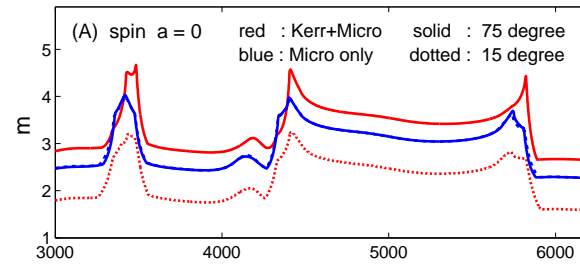
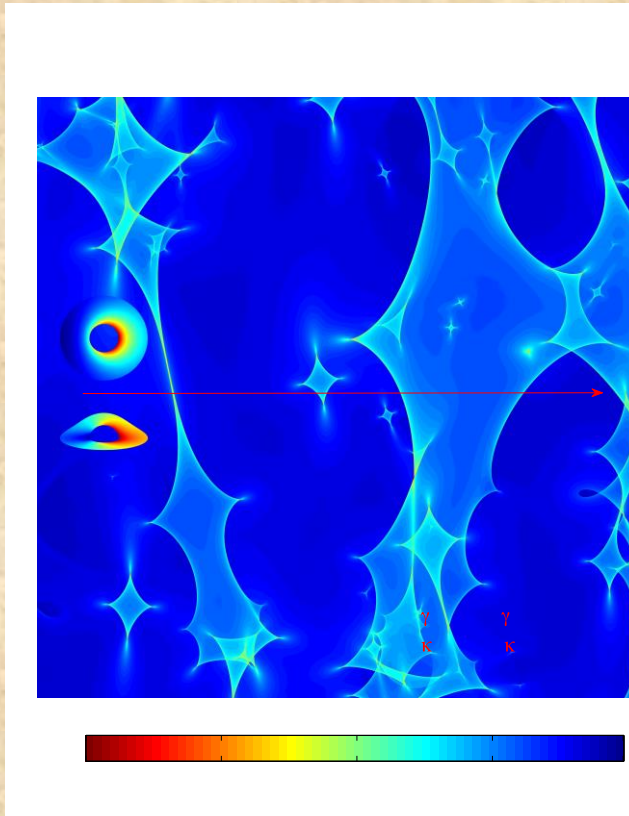
- Chen et al. 2013, ApJ, 762, 122.
- Poster 14x

Testing Unification Models

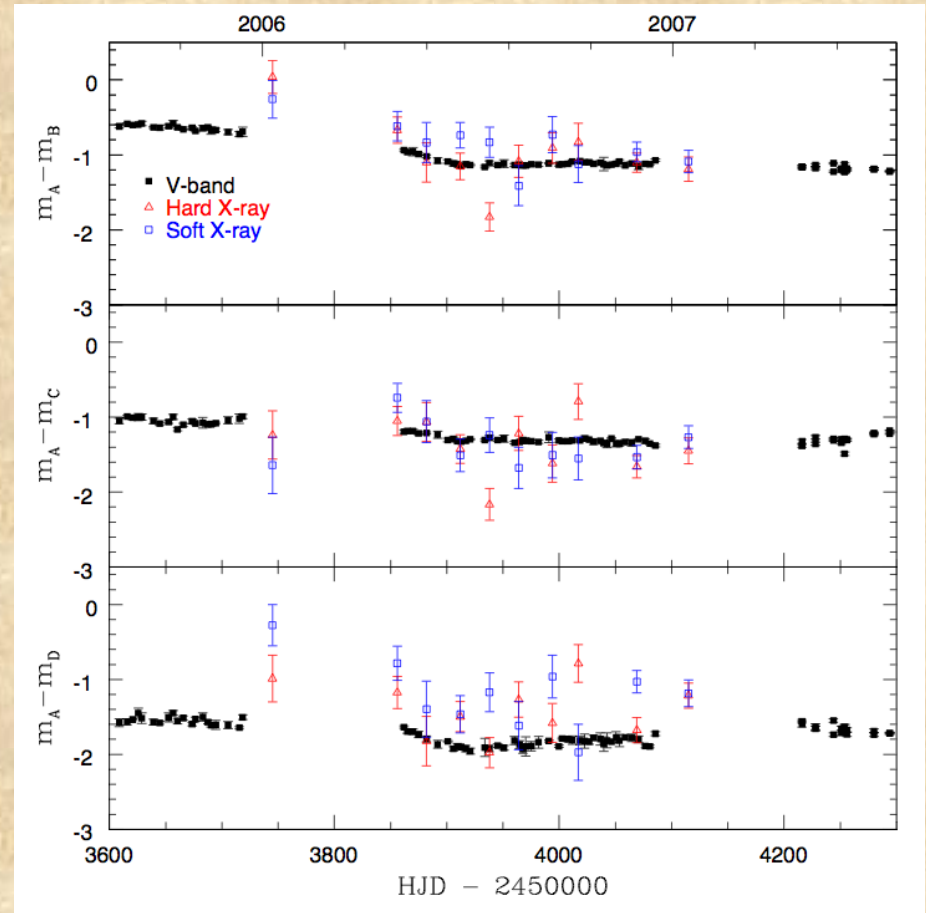
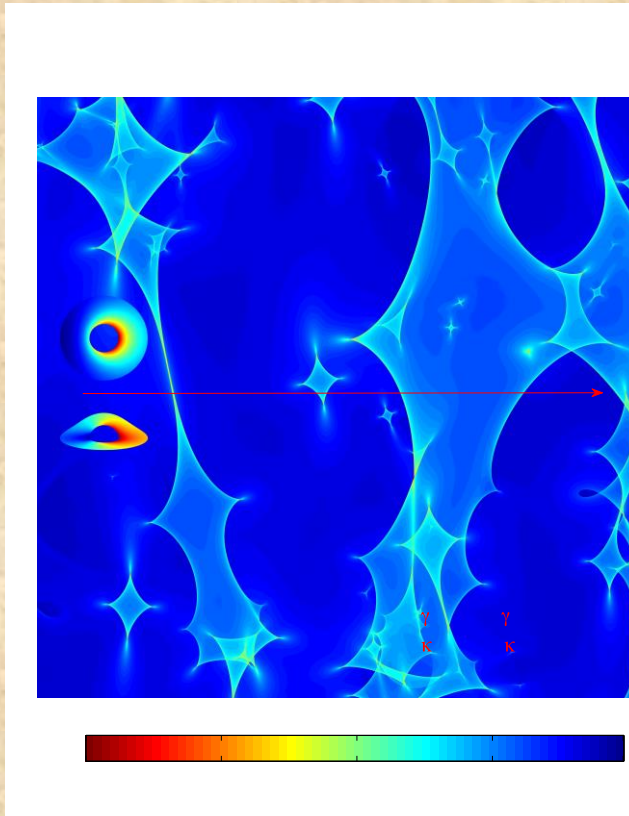


- Predicted aox distribution between BALs and non-BALs

Potential New Spin Measurement Technique



Potential New Spin Measurement Technique



Quasar Microlensing after Chandra Era

- Athena+: 2--2.5 m² effective area at 1 keV, 5--3'' angular resolution
- 10,000 Quasar-Galaxy lenses detected by DES, LSST, WFIRST
 - We will apply the technique to the large separation lens like SDSS1004.

